



# Acoustic scattering simulations in coupled fluid-porous media problems

---

Ashwin S. Nayak<sup>1,2</sup>, Andrés Prieto<sup>1,2</sup>, Daniel Fernández-Comesaña<sup>3</sup>  
Valencia, Spain – July 17, 2019

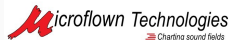
<sup>1</sup>Technological Institute of Industrial Mathematics, Spain

<sup>2</sup>University of A Coruña, Spain

<sup>3</sup>Microflown Technologies B.V, Netherlands



UNIVERSIDADE DA CORUÑA



Funded by the EU Horizon 2020 Research and Innovation programme under the Marie Skłodowska-Curie Grant No. 765374.

# Table of contents

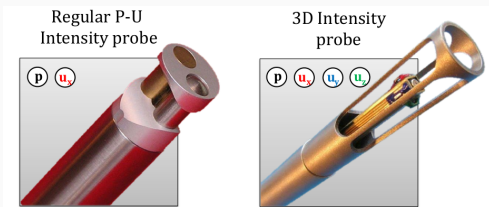
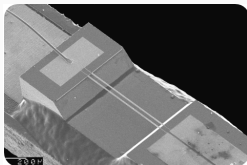
1. Introduction
2. Mathematical model
3. Benchmark case
4. Numerical results
5. Conclusions

# Introduction

---

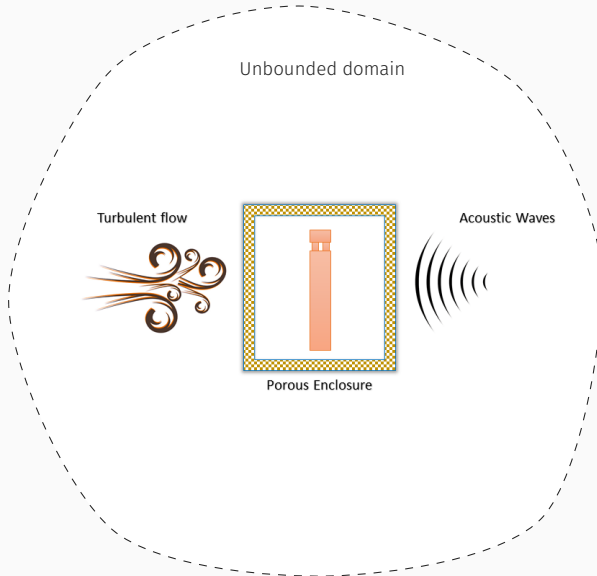
# Introduction : The Microflow

- Microflown PU probe is an acoustic sensor measuring particle velocity.
- Transducer designed on thermal principle
- Sensitive to fluid flow conditions
- Requires windscreens for wind velocities  $> 15$  m/s



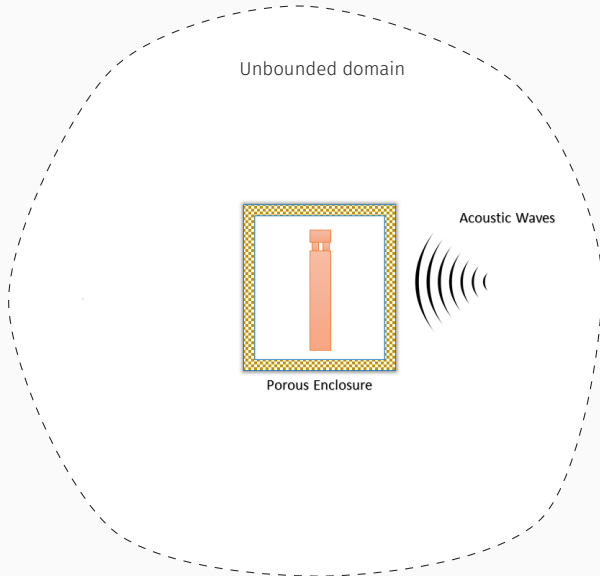
A microscopic view of the Microflow transducer (*left*), a regular PU probe (*middle*) and a 3D intensity probe (*right*)

# Main goal of the project



A schematic of the objective coupled problem

# Simplified problem setting

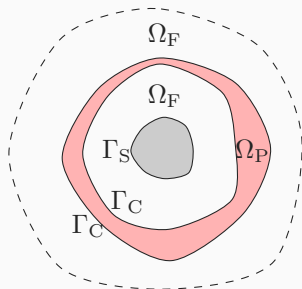


A schematic of the simplified coupled problem

# Mathematical model

---

# Mathematical model



General problem setting

For a given angular frequency  $\omega > 0$ :

$$-\nabla(\rho_F c_F^2 \operatorname{div} \mathbf{u}_F) - \rho_F \omega^2 \mathbf{u}_F = \mathbf{f}_F \quad \text{in } \Omega_F,$$

$$-\nabla(K_P(\omega) \operatorname{div} \mathbf{u}_P) - \rho_P(\omega) \omega^2 \mathbf{u}_P = \mathbf{f}_P \quad \text{in } \Omega_P,$$

$$\mathbf{u}_F \cdot \mathbf{n} = g \quad \text{on } \Gamma_S,$$

$$\mathbf{u}_F \cdot \mathbf{n} - \mathbf{u}_P \cdot \mathbf{n} = 0 \quad \text{on } \Gamma_C,$$

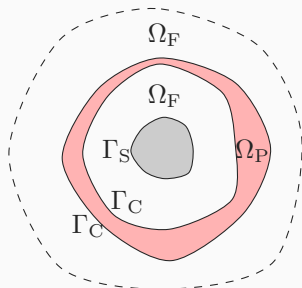
$$\rho_F c_F^2 \operatorname{div} \mathbf{u}_F - K_P(\omega) \operatorname{div} \mathbf{u}_P = 0 \quad \text{on } \Gamma_C,$$

$$\lim_{|\mathbf{x}| \rightarrow \infty} |\mathbf{x}| \left( \operatorname{div} \mathbf{u}_F - ik_F \mathbf{u}_F \cdot \frac{\mathbf{x}}{|\mathbf{x}|} \right) = \mathbf{0},$$

## Assumptions:

- Fluid: Homogeneous, non-viscous, compressible, isotropic, isentropic acoustic fluid
- Porous medium: Homogeneous, isotropic, isothermal porous material

# Mathematical model



General problem setting

For a given angular frequency  $\omega > 0$ :

$$-\nabla(\rho_F c_F^2 \operatorname{div} \mathbf{u}_F) - \rho_F \omega^2 \mathbf{u}_F = \mathbf{f}_F \quad \text{in } \Omega_F,$$

$$-\nabla(K_P(\omega) \operatorname{div} \mathbf{u}_P) - \rho_P(\omega) \omega^2 \mathbf{u}_P = \mathbf{f}_P \quad \text{in } \Omega_P,$$

$$\mathbf{u}_F \cdot \mathbf{n} = g \quad \text{on } \Gamma_S,$$

$$\mathbf{u}_F \cdot \mathbf{n} - \mathbf{u}_P \cdot \mathbf{n} = 0 \quad \text{on } \Gamma_C,$$

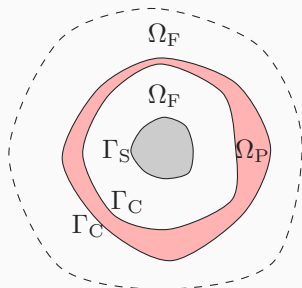
$$\rho_F c_F^2 \operatorname{div} \mathbf{u}_F - K_P(\omega) \operatorname{div} \mathbf{u}_P = 0 \quad \text{on } \Gamma_C,$$

$$\lim_{|\mathbf{x}| \rightarrow \infty} |\mathbf{x}| \left( \operatorname{div} \mathbf{u}_F - ik_F \mathbf{u}_F \cdot \frac{\mathbf{x}}{|\mathbf{x}|} \right) = \mathbf{0},$$

where

- $\Omega_F$ : fluid subdomain,  $\mathbf{f}_F$ : fluid source term
- $\Omega_P$ : porous subdomain,  $\mathbf{f}_P$ : porous source term
- $\Gamma_S$ : rigid solid boundary,  $g$ : structural normal displacement
- $\Gamma_C$ : coupled fluid-porous boundary

# Mathematical model



General problem setting

For a given angular frequency  $\omega > 0$ :

$$-\nabla(\rho_F c_F^2 \operatorname{div} \mathbf{u}_F) - \rho_F \omega^2 \mathbf{u}_F = \mathbf{f}_F \quad \text{in } \Omega_F,$$

$$-\nabla(K_P(\omega) \operatorname{div} \mathbf{u}_P) - \rho_P(\omega) \omega^2 \mathbf{u}_P = \mathbf{f}_P \quad \text{in } \Omega_P,$$

$$\mathbf{u}_F \cdot \mathbf{n} = g \quad \text{on } \Gamma_S,$$

$$\mathbf{u}_F \cdot \mathbf{n} - \mathbf{u}_P \cdot \mathbf{n} = 0 \quad \text{on } \Gamma_C,$$

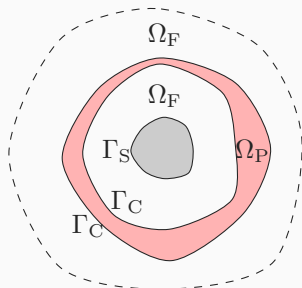
$$\rho_F c_F^2 \operatorname{div} \mathbf{u}_F - K_P(\omega) \operatorname{div} \mathbf{u}_P = 0 \quad \text{on } \Gamma_C,$$

$$\lim_{|\mathbf{x}| \rightarrow \infty} |\mathbf{x}| \left( \operatorname{div} \mathbf{u}_F - ik_F \mathbf{u}_F \cdot \frac{\mathbf{x}}{|\mathbf{x}|} \right) = \mathbf{0},$$

where

- $\mathbf{u}_F, \mathbf{u}_P$ : fluid and porous displacement field
- $\rho_F, \rho_P(\omega)$ : fluid and dynamic porous mass density
- $c_F$ : fluid sound speed
- $K_P(\omega)$ : dynamic porous bulk modulus

# Mathematical model



General problem setting

For a given angular frequency  $\omega > 0$ :

$$-\nabla(\rho_F c_F^2 \operatorname{div} \mathbf{u}_F) - \rho_F \omega^2 \mathbf{u}_F = \mathbf{f}_F \quad \text{in } \Omega_F,$$

$$-\nabla(K_P(\omega) \operatorname{div} \mathbf{u}_P) - \rho_P(\omega) \omega^2 \mathbf{u}_P = \mathbf{f}_P \quad \text{in } \Omega_P,$$

$$\mathbf{u}_F \cdot \mathbf{n} = g \quad \text{on } \Gamma_S,$$

$$\mathbf{u}_F \cdot \mathbf{n} - \mathbf{u}_P \cdot \mathbf{n} = 0 \quad \text{on } \Gamma_C,$$

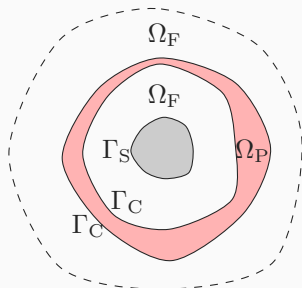
$$\rho_F c_F^2 \operatorname{div} \mathbf{u}_F - K_P(\omega) \operatorname{div} \mathbf{u}_P = 0 \quad \text{on } \Gamma_C,$$

$$\lim_{|\mathbf{x}| \rightarrow \infty} |\mathbf{x}| \left( \operatorname{div} \mathbf{u}_F - ik_F \mathbf{u}_F \cdot \frac{\mathbf{x}}{|\mathbf{x}|} \right) = \mathbf{0},$$

where

- $\mathbf{u}_F, \mathbf{u}_P$ : fluid and porous displacement field
- $\rho_F, \rho_P(\omega)$ : fluid and dynamic porous mass density
- $c_F$ : fluid sound speed
- $K_P(\omega)$ : dynamic porous bulk modulus

# Mathematical model



General problem setting

For a given angular frequency  $\omega > 0$ :

$$-\nabla(\rho_F c_F^2 \operatorname{div} \mathbf{u}_F) - \rho_F \omega^2 \mathbf{u}_F = \mathbf{f}_F \quad \text{in } \Omega_F,$$

$$-\nabla(K_P(\omega) \operatorname{div} \mathbf{u}_P) - \rho_P(\omega) \omega^2 \mathbf{u}_P = \mathbf{f}_P \quad \text{in } \Omega_P,$$

$$\mathbf{u}_F \cdot \mathbf{n} = g \quad \text{on } \Gamma_S,$$

$$\mathbf{u}_F \cdot \mathbf{n} - \mathbf{u}_P \cdot \mathbf{n} = 0 \quad \text{on } \Gamma_C,$$

$$\rho_F c_F^2 \operatorname{div} \mathbf{u}_F - K_P(\omega) \operatorname{div} \mathbf{u}_P = 0 \quad \text{on } \Gamma_C,$$

$$\lim_{|\mathbf{x}| \rightarrow \infty} |\mathbf{x}| \left( \operatorname{div} \mathbf{u}_F - ik_F \mathbf{u}_F \cdot \frac{\mathbf{x}}{|\mathbf{x}|} \right) = \mathbf{0},$$

where

- $\mathbf{u}_F, \mathbf{u}_P$ : fluid and porous displacement field
- $\rho_F, \rho_P(\omega)$ : fluid and dynamic porous mass density
- $c_F$ : fluid sound speed
- $K_P(\omega)$ : dynamic porous bulk modulus

# Fluid-equivalent porous model

## Johnson-Champoux-Allard-Lafarge (JCAL) model

- Valid for porous materials with arbitrarily shaped pores
- Six-parameter model to describe rigid-frame porous media properties

Parameter	#	Value
Porosity	$\phi$	0.94
Flow Resistivity	$\sigma$	4e4
Tortuosity	$\alpha_\infty$	1.06
Viscous Characteristic Length	$\Lambda$	56e-6
Thermal Characteristic Length	$\Lambda'$	110e-6
Static Thermal Permeability	$k_0'$	2.5e-10

The model also involves the fluid mass density  $\rho_F$ , specific heat ratio  $\gamma$ , Prandtl Number  $Pr$ , and equilibrium fluid pressure  $P_F$

# Fluid-equivalent porous model

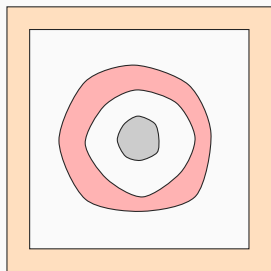
## Johnson-Champoux-Allard-Lafarge (JCAL) model

- Valid for porous materials with arbitrarily shaped pores
- Six-parameter model to describe rigid-frame porous media properties

$$\rho_P(\omega) = \frac{\rho_F}{\phi} \alpha_\infty \left( 1 - i \frac{\sigma \phi}{\omega \rho_F \alpha_\infty} \sqrt{1 + i \frac{4\alpha_\infty^2 \eta \rho_F \omega}{\sigma^2 \Lambda^2 \phi^2}} \right),$$
$$K_P(\omega) = \frac{\gamma P_F / \phi}{\gamma - (\gamma - 1) \left( 1 - i \frac{\eta \phi}{\rho_F k'_0 \omega \text{Pr}} \sqrt{1 + i \frac{4k'_0{}^2 \rho_F \omega \text{Pr}}{\eta \Lambda'^2 \phi^2}} \right)^{-1}},$$

The model also involves the fluid mass density  $\rho_F$ , specific heat ratio  $\gamma$ , Prandtl Number  $\text{Pr}$ , and equilibrium fluid pressure  $P_F$

# Perfectly Matched Layers (PML) technique



$\square \Omega_F$     $\square \Omega_P$     $\square \Omega_{PML}$

Schematic of PML Model

- Truncate the domain at some finite distance
- Wrap by an absorption layer  $\Omega_{PML}$ ,
  - Involve complex-valued stretching of the spatial coordinates:

$$\tilde{\nabla} \phi = \sum_{j=1}^3 \frac{1}{\gamma_j} \frac{\partial \phi}{\partial x_j} \mathbf{e}_j,$$

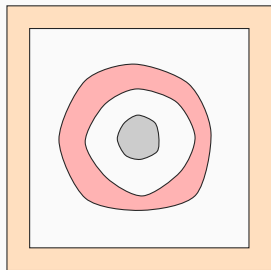
$$\tilde{\text{div}} \mathbf{w} = \sum_{j=1}^3 \frac{1}{\gamma_j} \frac{\partial w_j}{\partial x_j},$$

with  $\gamma_j \in \mathbb{C}$ ,  $j = 1, 2, 3$ .



Bermúdez A., Hervella-Nieto L. M., Prieto A., Rodríguez R., "An optimal perfectly matched layer with unbounded absorbing function for time-harmonic acoustic scattering problems", J. Comput. Phys., 223, 469-48, 2007

# Perfectly Matched Layers (PML) technique



$\square \Omega_F$     $\square \Omega_P$     $\square \Omega_{PML}$

Schematic of PML Model

$$\Omega_{PML} = \prod_{j=1}^3 [-L_j^\infty, L_j^\infty] \setminus \prod_{j=1}^3 [-L_j, L_j]$$

$\gamma_j \in \mathbb{C}$ ,  $j = 1, 2, 3$  are modeled by a piecewise smooth function,

$$\gamma_j(x_j) = \begin{cases} 1 & |x_j| \leq L_j, \\ 1 + i\sigma_j(x_j) & L_j \leq |x_j| \leq L_j^\infty, \end{cases}$$

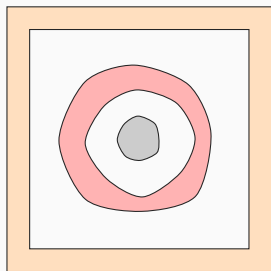
with  $\sigma_j(x_j) = c_F / (\omega(L_j^\infty - |x_j|))$

- Singular on boundary
- Optimally tuned to absorb waves of any frequency



Bermúdez A., Hervella-Nieto L. M., Prieto A., Rodríguez R., “An optimal perfectly matched layer with unbounded absorbing function for time-harmonic acoustic scattering problems”, J. Comput. Phys., 223, 469-48, 2007

# Perfectly Matched Layers (PML) technique



$\square \Omega_F$     $\square \Omega_P$     $\square \Omega_{PML}$

Schematic of PML Model

The governing (PML) equation in  $\Omega_{PML}$ :

$$-\tilde{\nabla}(\rho_{PML} c_F^2 \tilde{\text{div}} \mathbf{u}_{PML}) - \rho_F \omega^2 \mathbf{u}_{PML} = \mathbf{0},$$

or, in an equivalent form,

$$-\text{div}(\rho_F c_F^2 \tilde{\mathbf{C}}(\nabla \mathbf{u}_{PML})) - \rho_F \omega^2 \tilde{\mathbf{M}} \mathbf{u}_{PML} = \mathbf{0},$$

where

$$\text{4th order tensor: } \tilde{\mathbf{C}}(\nabla \mathbf{w}) = (\tilde{\text{div}} \mathbf{w}) \mathbf{I},$$

$$\text{2nd order tensor: } \tilde{\mathbf{M}} = \sum_{j=1}^3 \gamma_j \mathbf{e}_j \otimes \mathbf{e}_j.$$



Bermúdez A., Hervella-Nieto L. M., Prieto A., Rodríguez R., “An optimal perfectly matched layer with unbounded absorbing function for time-harmonic acoustic scattering problems”, J. Comput. Phys., 223, 469-48, 2007

# Planewave scattering problem

Total fields are decomposed in incident and scattering fields:  $\mathbf{u}_F = \mathbf{u}_F^{\text{inc}} + \mathbf{u}_F^{\text{sc}}$  with

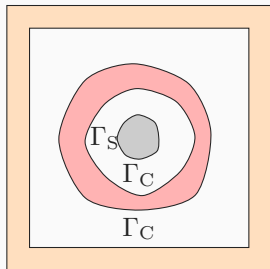
$$\mathbf{u}_F^{\text{inc}} = \frac{1}{\rho_F \omega^2} \nabla (A_F \exp(\mathbf{k}_F \cdot \mathbf{x})), \quad |\mathbf{k}_F| = \omega / c_F.$$

- $\mathbf{u}_F^{\text{inc}}$  is a solution of Helmholtz-like equation in  $\Omega_F$ :

$$-\nabla(\rho_F c^2 \operatorname{div} \mathbf{u}_F^{\text{inc}}) - \rho_F \omega^2 \mathbf{u}_F^{\text{inc}} = \mathbf{0},$$

- but *not* in the porous subdomain  $\Omega_P$ , where  $\mathbf{u}_P = \mathbf{u}_P^{\text{sc}} + \mathbf{u}_P^{\text{inc}}$ , so

$$-\nabla(K_P(\omega) \operatorname{div} \mathbf{u}_P^{\text{inc}}) - \rho_P(\omega) \omega^2 \mathbf{u}_P^{\text{inc}} = \mathbf{f}_P \neq \mathbf{0}.$$



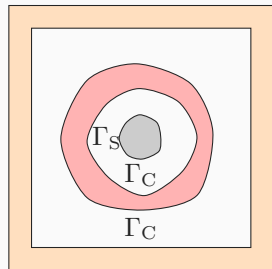
$\square \Omega_F$      $\square \Omega_P$      $\square \Omega_{\text{PML}}$

Schematic of Final Model

# Planewave scattering problem

Since the normal components of displacement fields are continuous across interfaces, the scattering displacement field is defined as,

$$\mathbf{u} = \begin{cases} \mathbf{u}_F^{\text{sc}} & \text{in } \Omega_F, \\ \mathbf{u}_P^{\text{sc}} & \text{in } \Omega_P, \\ \mathbf{u}_{\text{PML}} & \text{in } \Omega_{\text{PML}}. \end{cases}$$



$\square \Omega_F$     $\square \Omega_P$     $\square \Omega_{\text{PML}}$

Schematic of Final Model

# Variational Formulation

Introduce  $\Omega = \Omega_F \cup \Omega_P \cup \Omega_{PML}$  and the functional space

$$\mathbf{V} = \left\{ \mathbf{v} \in [L^2(\Omega)]^3 : \begin{array}{l} \mathbf{v}|_{\Omega_F} \in \mathbf{H}(\text{div}, \Omega_F), \mathbf{v}|_{\Omega_P} \in \mathbf{H}(\text{div}, \Omega_P), \\ \widetilde{\mathbf{M}}\mathbf{v}|_{\Omega_{PML}} \in [L^2(\Omega_{PML})]^3, \widetilde{\text{div}}(\mathbf{v}|_{\Omega_{PML}}) \in L^2(\Omega_{PML}), \\ \mathbf{v} \cdot \mathbf{n} = 0 \text{ on } \Gamma_\infty \end{array} \right\}$$

## Variational problem

Given  $\omega > 0$ , find  $\mathbf{u} \in \mathbf{V}$  such that  $\mathbf{u} \cdot \mathbf{n} = -\mathbf{u}_F^{\text{inc}} \cdot \mathbf{n}$  on  $\Gamma_S$ , and

$$\left. \begin{array}{l} \int_{\Omega_F} \rho_F c^2 (\text{div } \mathbf{u})(\text{div } \mathbf{v}) \, dV - \int_{\Omega_F} \rho_F \omega^2 \mathbf{u} \cdot \mathbf{v} \, dV \\ + \int_{\Omega_P} \mathbf{K}_P(\omega) (\text{div } \mathbf{u})(\text{div } \mathbf{v}) \, dV - \int_{\Omega_P} \rho_P(\omega) \omega^2 \mathbf{u} \cdot \mathbf{v} \, dV \\ + \int_{\Omega_{PML}} \rho_F c^2 \widetilde{\mathbf{C}}(\nabla \mathbf{u}) : \nabla \mathbf{v} \, dV - \int_{\Omega_{PML}} \rho_F \omega^2 \widetilde{\mathbf{M}} \mathbf{u} \cdot \mathbf{v} \, dV \end{array} \right\} = \int_{\Omega_P} \mathbf{f}_P \cdot \mathbf{v} \, dV,$$

for all  $\mathbf{v} \in \mathbf{V}$  with  $\mathbf{v} \cdot \mathbf{n} = 0$  on  $\Gamma_S$ .

We discretize using the first-order Raviart-Thomas Finite Elements ( $\mathbf{RT}_h^1$ ) over a tetrahedral mesh  $\mathcal{T}_h$  of  $\Omega$ ,

## Raviart-Thomas Finite Element Space

$$\mathbf{RT}_h^1(\Omega) = \left\{ \mathbf{v} \in \mathbf{H}(\text{div}, \Omega) : \mathbf{v}|_T = \mathbf{a} + b\mathbf{x}, \mathbf{a} \in \mathbb{C}^3, b \in \mathbb{C}, T \in \mathcal{T}_h \right\}$$

- Constant divergence in each element
- Constant normal component on all faces of tetrahedra
- Completely determined if their normal components are known on each face.

**Pressure fields** are computed from the fluid and porous displacement field:

$$\begin{aligned}p_{\text{F}} &= -\rho_{\text{F}} c^2 \operatorname{div} \mathbf{u}_{\text{F}} \quad \text{in } \Omega_{\text{F}}, \\p_{\text{P}} &= -K_{\text{P}}(\omega) \operatorname{div} \mathbf{u}_{\text{P}} \quad \text{in } \Omega_{\text{P}}.\end{aligned}$$

Since  $\mathbf{u}_{\text{F}}^h \in \mathbf{RT}_h^1(\Omega_{\text{F}})$  and  $\mathbf{u}_{\text{P}}^h \in \mathbf{RT}_h^1(\Omega_{\text{P}})$ ,  
the numerical approximation for induced pressure fields:  
 $p_{\text{F}}^h \in \mathbf{DG}_h^0(\Omega_{\text{F}})$  and  $p_{\text{P}}^h \in \mathbf{DG}_h^0(\Omega_{\text{P}})$ .

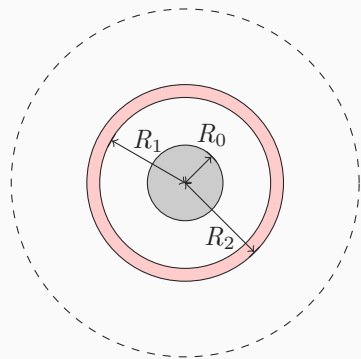
**3D Directivity patterns** are also computed by evaluating pressure fields at uniformly distributed points on a sphere,  $\mathbf{m}_j, j = 1, \dots, M$ :

$$\text{Directivity}^h(\mathbf{m}_j) = \frac{|p_{\text{F}}^h(\mathbf{m}_j)| - \min_{\mathbf{m}_j} |p_{\text{F}}^h(\mathbf{m}_j)|}{\|p_{\text{F}}^h\|_{\text{L}^\infty(\Omega_{\text{F}})} - \min_{\mathbf{m}_j} |p_{\text{F}}^h(\mathbf{m}_j)|}.$$

## Benchmark case

---

# Benchmark case : Monopole



□  $\Omega_F$     ■  $\Omega_P$

Schematic of the benchmark  
monopole case

For a given  $\omega > 0$ , writing the problems in term of pressure fields we obtain the exact solution:

$$p_1(r) = A_1 \frac{e^{-ik_F r}}{r} + B_1 \frac{e^{ik_F r}}{r}, \quad r \in [R_0, R_1],$$

$$p_2(r) = A_2 \frac{e^{-ik_P r}}{r} + B_2 \frac{e^{ik_P r}}{r}, \quad r \in [R_1, R_2],$$

$$p_3(r) = B_3 \frac{e^{ik_F r}}{r}, \quad r \in [R_2, \infty),$$

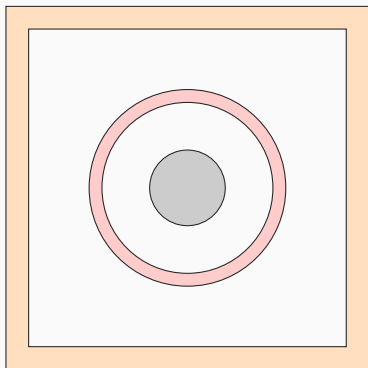
with boundary conditions

$$p'(R_0) = \rho_F \omega^2 g_0, \quad g_0 = \text{constant},$$

$$p_1(R_1) = p_2(R_1), \quad \rho_P p'_1(R_1) = \rho_F p'_2(R_1),$$

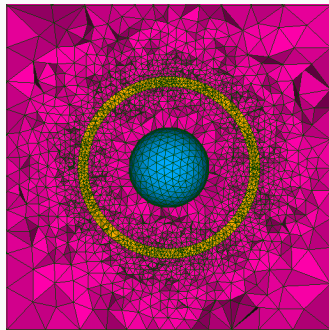
$$p_2(R_2) = p_3(R_2), \quad \rho_F p'_2(R_2) = \rho_P p'_3(R_2).$$

# Benchmark case: Implementation



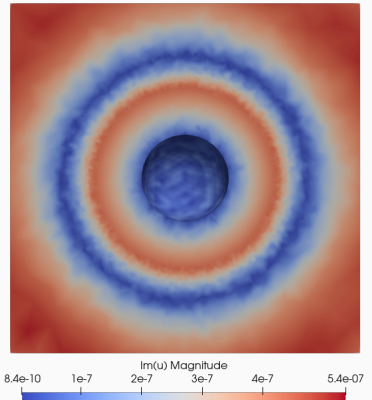
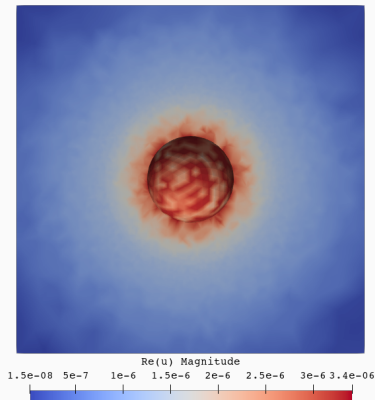
$\square \Omega_F$     $\square \Omega_P$     $\square \Omega_{PML}$

Schematic of Benchmark case (left) and snapshot of mesh(right).  
The PML layer is not shown in mesh.



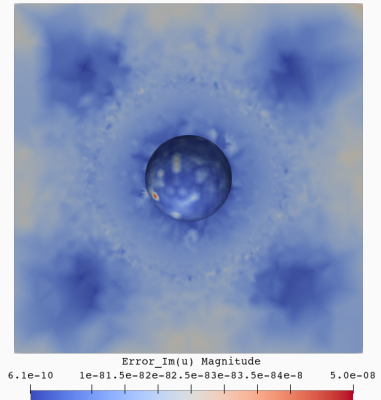
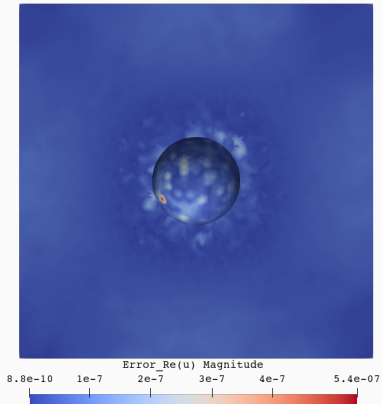
- Conformal mesh in subdomains and coupling boundaries
- Local refinements around the porous layer and the rigid solid

# Benchmark case: Displacement Field



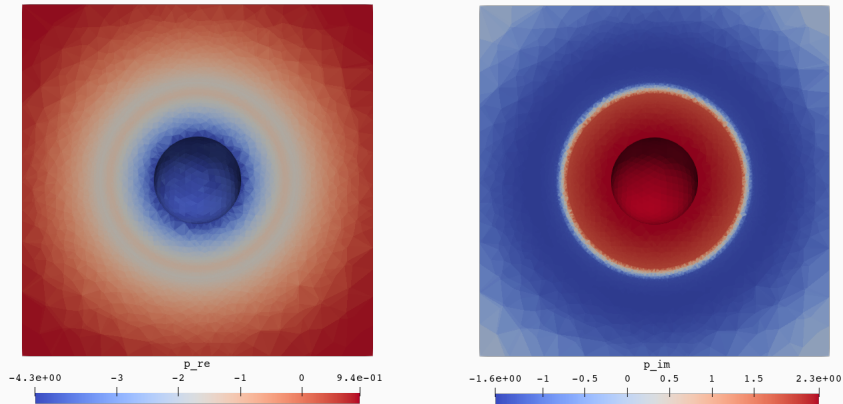
The computed real (*left*) and imaginary (*right*) parts of displacement field. The field is qualitatively uniform the radial directions with aberrations due to interpolations in a non-uniform mesh.

# Benchmark case: Displacement Field



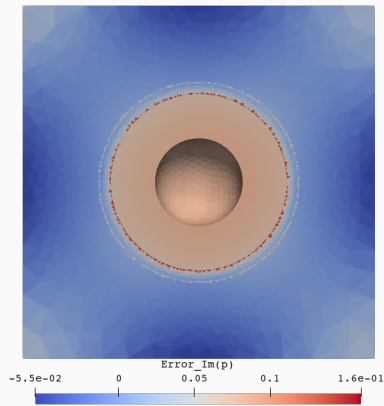
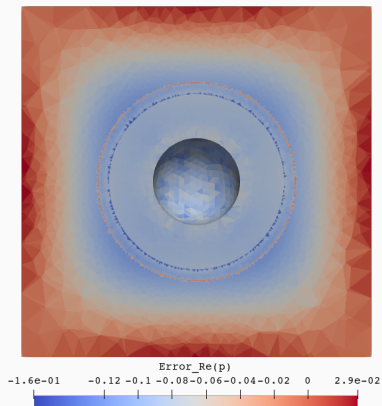
The computed real (*left*) and imaginary (*right*) parts of errors in displacement field. The errors are mostly minimal in orders of magnitude of the displacement field.

# Benchmark case: Pressure Field



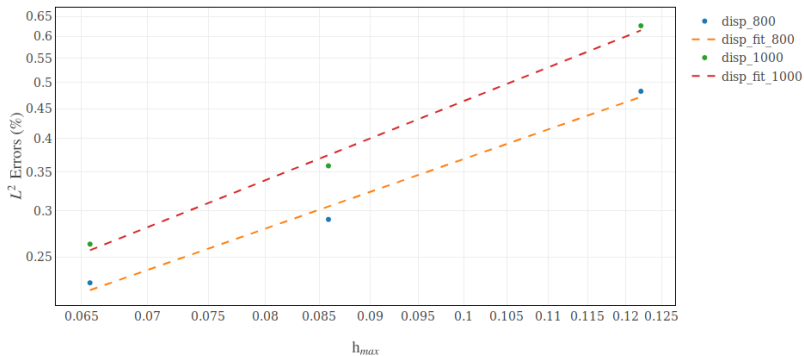
The computed real (*left*) and imaginary (*right*) parts of the pressure field.  
The field is qualitatively uniform along the radial directions.

# Benchmark case: Pressure field



The computed real (*left*) and imaginary (*right*) parts of the errors in the pressure field. The field is qualitatively agreeable with the errors smaller by an order of magnitude.

# Benchmark case: Error Convergence



Slopes of fitted lines: 1.2370 (800Hz) and 1.41 (1000Hz)

$$L^2\text{-rel. error (\%)} = 100 \frac{\|\mathbf{u} - \mathbf{u}_{ex}\|_{L^2(\Omega_F)}}{\|\mathbf{u}_{ex}\|_{L^2(\Omega_F)}}$$

## Numerical results

---

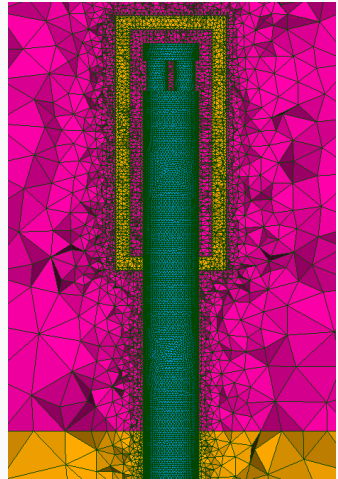
# Scenario

## Mesh Information

- # Elements: 902971
- # Vertices: 169633
- Conformal with layers
- Local refinements

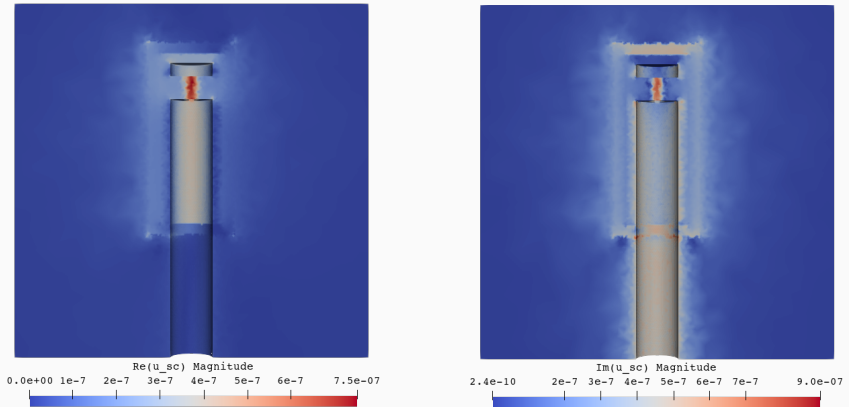
Frequency = 800Hz

Incident Planewave in the  $+x$  direction.



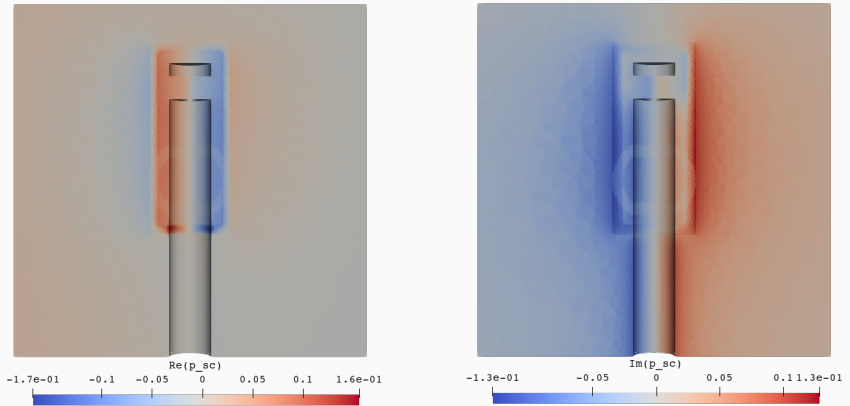
Snapshot of the PU Probe Mesh cross-section. Only the bottom PML layer is partly visible.

# Results: Scattered Displacement Field



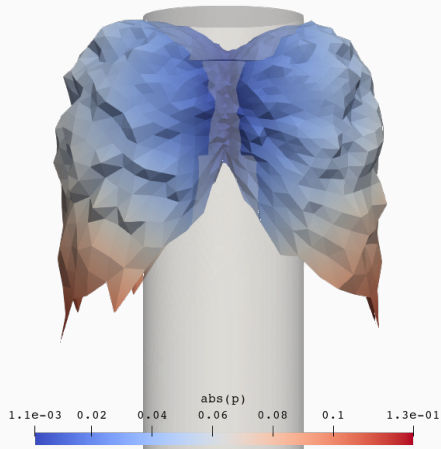
The real (*left*) and imaginary (*right*) parts of the scattered displacement field. The field clearly shows higher displacement amplitudes between the probe pillars. Also visible are acoustic dispersions at corners of the porous layers.

# Results: Scattered Pressure Field



The computed real (*left*) and imaginary (*right*) parts of the scattered pressure field. The field clearly shows scatter behaviour of the plane wave along direction of propagation.

# Directivity



The computed directivity of the scattered pressure field.

The plot allows for highlighting directions of influence by the scattering object.

# Conclusions

---

# Conclusions

- A mathematical model has been developed for coupling porous layers and deal with radiating boundary conditions
- The model has been validated
- A customizable tool has been developed which lets deeper insights in sensor design
  - Prototyping different porous-layer configurations
- Frequency response studies and other analysis is made available.

Thank You!